Elastic Scattering of C^{12} Ions from Fe, Ni, Ag^{107}, In, and Ta*

JONAS ALSTER†
Lawrence Radiation Laboratory, University of California, Berkeley, California
and
Physics Department, University of Washington, Seattle, Washington

AND

HOMER E. CONZETT
Lawrence Radiation Laboratory, University of California, Berkeley, California

(Received 29 June 1964)

The angular distributions of C^{12} ions elastically scattered from Fe, Ni, Ag^{107}, In, and Ta have been measured at an energy of 124.5 MeV. The experimental data were analyzed using a parameterized phase-shift analysis. Very good agreement with experiment was obtained. Precise values for absorption radii, surface parameters, and total reaction cross section could be extracted.

I. INTRODUCTION

ELASTIC scattering experiments utilizing beams of heavy ions[1–7] have been very useful in providing quite precise information on such parameters as the radii and surface thicknesses of the regions of "interaction" between the colliding complex nuclei. This has been possible because of two conditions whose importance has recently been more clearly appreciated.[8–10] That is, this type of scattering is characterized (1) by strong absorption of those partial waves corresponding to trajectories which penetrate the interaction region, and (2) by the large number of partial waves which contribute to the scattering. The treatment of the scattering data in terms of parameterized phase-shift analyses has provided both excellent agreement between calculation and experiment, and a clear physical interpretation of the parameters used. We include here all analyses[9–13] in which the partial-wave (complex) phase shifts are explicit parameters in the calculation and are not adjusted through an intermediary complex potential. Thus, one works directly with the scattering amplitude and finds it unnecessary, for example, to ascribe any basic physical significance to the single-particle complex-potential description[14] of the scattering of "particles" (e.g., deuterons, alpha particles, heavy ions) whose existence within the interaction region is questionable.

The parameterized phase-shift analysis is completely phenomenological. The differential cross section for elastic scattering is $\sigma(\theta)=|f(\theta)|^2$, with the scattering amplitude given by

$$f(\theta)=f_c(\theta)+\frac{i}{2k}\sum_{l=0}^{\infty}(2l+1)e^{2i\sigma_l}(1-A_l e^{2i\delta_l})P_l(\cos\theta), \quad (1)$$

where $f_c(\theta)$ is the (point-charge) Coulomb scattering amplitude, $\sigma_l=\arg\Gamma(1+l+in)$ with $n=Z_1Z_2e^2/\hbar v$, A_l is the amplitude of the outgoing lth partial wave, and δ_l is its (real) nuclear phase shift. Thus, $0\leq A_l\leq 1$, with $A_l=1$ corresponding to no absorption and $A_l=0$, to complete absorption. McIntyre *et al.*[12] introduced the (arbitrary) forms

$$A_l=1-\left[1+\exp\frac{l-l_A}{\Delta l_A}\right]^{-1}, \quad \delta_l=\delta\left[1+\exp\frac{l-l_\delta}{\Delta l_\delta}\right]^{-1} \quad (2)$$

---

* This paper is based on a thesis submitted to the Technical University of Delft, The Netherlands, in partial fulfillment of the Ph.D. degree—University of California Lawrence Radiation Laboratory report UCRL-9650, 1961 (unpublished). This work was done under the auspices of the U. S. Atomic Energy Commission.

† Present address: Department of Physics, University of Washington, Seattle, Washington.

[1] H. L. Reynolds and A. Zucker, Phys. Rev. **102**, 1378 (1956).
[2] E. Goldberg and H. L. Reynolds, Phys. Rev. **112**, 1981 (1958).
[3] M. L. Halbert and A. Zucker, Phys. Rev. **115**, 1635 (1959).
[4] J. A. McIntyre, S. D. Baker, and T. L. Watts, Phys. Rev. **116**, 1212 (1959).
[5] H. L. Reynolds, E. Goldberg, and D. D. Kerlee, Phys. Rev. **119**, 2009 (1960); D. D. Kerlee, H. L. Reynolds, and E. Goldberg, *ibid.* **127**, 1224 (1962).
[6] J. Alster and H. E. Conzett, *Proceedings of the Second Conference on Reactions between Complex Nuclei*, edited by A. Zucker, E. C. Halbert, and F. T. Howard (John Wiley & Sons, Inc., New York, 1960), p. 175.
[7] J. A. McIntyre, S. D. Baker, and K. H. Wang, Phys. Rev. **125**, 584 (1962).
[8] J. Alster, University of California, Lawrence Radiation Laboratory Report UCRL-9650, 1961 (unpublished).
[9] W. E. Frahn and R. H. Venter, Ann. Phys. (N.Y.) **24**, 243 (1963).
[10] H. E. Conzett, A. Isoya, and E. Hadjimichael, in *Proceedings of the Third Conference on Reactions between Complex Nuclei*, edited by A. Ghiorso, R. M. Diamond, and H. E. Conzett (University of California Press, Berkeley, 1963).
[11] J. S. Blair, Phys. Rev. **95**, 1218 (1954).
[12] J. A. McIntyre, K. H. Wang, and L. C. Becker, Phys. Rev. **117**, 1337 (1960).
[13] Applications to high-energy nucleon scattering are developed by K. R. Greider and A. E. Glassgold, Ann. Phys. (N. Y.) **10**, 100 (1960), and by L. R. B. Elton, Nucl. Phys. **23**, 681 (1961).
[14] For alpha particles, George Igo, Phys. Rev. **115**, 1665 (1959) and references therein. For deuterons, E. C. Halbert, Nucl. Phys. **50**, 353 (1964) and references therein. For heavy ions, C. E. Porter, Phys. Rev. **112**, 1722 (1958); R. H. Bassel and R. M. Drisko, in *Proceedings International Conference on Nuclear Structure, Kingston, Canada*, edited by D. A. Bromley and E. W. Vogt (University of Toronto Press, Toronto, 1960); E. H. Auerbach and C. E. Porter, *Proceedings of the Third Conference on Reactions between Complex Nuclei*, edited by A. Ghiorso, R. M. Diamond, and H. E. Conzett (University of California Press, Berkeley, 1963).

as an improvement over the "sharp cutoff" model[11] in fitting alpha-particle scattering data, and these forms subsequently provided excellent fits to heavy ion results.[6,7] The basic conditions of strong absorption and the participation of many partial waves underlie Eqs. (2). Because of the classical nature of the heavy-ion trajectories for $n\gg1$ and $kR\gg1$,[15] where R is the radius of the interaction region and $\hbar\mathbf{k}$ is the relative momentum, one can make the correspondence between l and r, the distance of closest approach for a particle of orbital angular momentum $[l(l+1)]^{1/2}\hbar$, through the relation

$$E=\frac{Z_1Z_2e^2}{r}+\frac{l(l+1)\hbar^2}{2\mu r^2}, \tag{3}$$

which can be rearranged to

$$kr=n+[n^2+l(l+1)]^{1/2}, \tag{4}$$

where $k=(1/\hbar)(2\mu E)^{1/2}$, and for $l\gg n$, Eq. (4) can be approximated by

$$kr\simeq n+(l+\tfrac{1}{2}).$$

Under these conditions, one can make the correspondence between coordinate (r) space and orbital angular momentum (l) space through equation (4), and we indicate this correspondence by writing $A_l(r)$. Since the value of r for which $A_l(r)=\frac{1}{2}$ is usually quoted as the "interaction" radius in this type of analysis, we shall call it the absorption radius R_a, since this terminology explicitly defines the method by which the determination was made. The corresponding radius parameter, r_a, is defined by $R_a=r_a(A_1^{1/3}+A_2^{1/3})$. Similarly, the absorption surface thickness S is taken to be the interval in r space over which $A_l(r)$ goes from 0.9 to 0.1, and so corresponds, through Eq. (2), to $4.4\Delta l_A$. The corresponding surface thickness parameter, $t=S/4.4$, is analogous to the complex potential surface parameter a.

Since values of $(kR_a)\gg1$ are available in the scattering of heavy-ion beams from the Berkeley HILAC,[16] these beams provide the means for precise determinations of the absorption parameters r_a and t. The experiments reported here had that objective, so most of the data were taken with counting statistics of 1% or better.

From Eq. (1), the ratio of $\sigma(\theta)$ to that for Coulomb scattering, $\sigma_c(\theta)$, is given by

$$\frac{\sigma(\theta)}{\sigma_c(\theta)}=\left|ie^{-in\ \ln[\sin^2(\frac{1}{2}\theta)]}+\frac{\sin^2(\frac{1}{2}\theta)}{n}\sum_{l=0}^{\infty}(2l+1)e^{2i(\sigma_l-\sigma_0)}\times(1-A_le^{2i\delta l})P_l(\cos\theta)\right|^2. \tag{5}$$

Calculation of this expression, with the parameterization of A_l and δ_l given by (2), was programmed for an IBM-704 computer, and minimum values of

$$\Delta\equiv\sum_i\frac{\sigma(\theta_i)_{\rm calc}-\sigma(\theta_i)_{\rm exp}}{\sigma(\theta_i)_{\rm exp}}\times100$$

were sought.

II. EXPERIMENTAL PROCEDURE

The scattering experiments were done with C^{12} ions, accelerated to their full energy of 124.5 MeV. After leaving the machine they were magnetically deflected and brought into a 10-in. scattering chamber, through two sets of collimators that define a $\frac{1}{8}$-in.-diam beam. Figure 1 shows the experimental arrangement. The target was placed at the center of the chamber, perpendicular to the beam. After passing through the target, the beam was stopped in a Faraday cup. The scattered particles left the chamber through a 0.002-in.

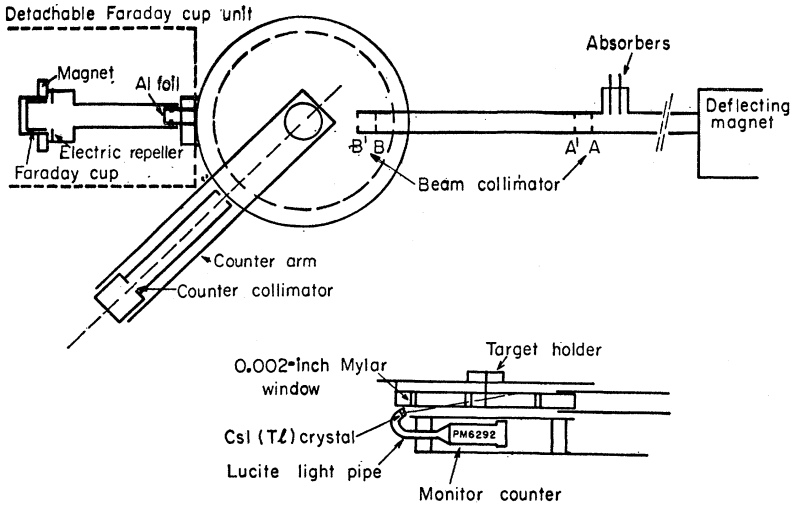

FIG. 1. Schematic top view and side view of the scattering chamber and monitor.

[15] E. J. Williams, Rev. Mod. Phys. **17**, 217 (1945).
[16] E. L. Hubbard, W. R. Baker, K. W. Ehlers, H. S. Gordon, R. M. Main *et al.*, Rev. Sci. Instr. **32**, 621 (1961).

Mylar window. The Faraday cup unit could be detached from the chamber and replaced by a flange with a 0.001-in.-thick aluminum-alloy vacuum window; this permitted the counters to reach laboratory scattering angles as small as 6 deg. The beam could still be monitored with a counter, mounted at a fixed angle (14 deg). The monitor counter was used in all experiments with or without the Faraday cup.

In the early stages of the experiment the counters consisted of a thin CsI(Tl) crystal, mounted on a Dumont-6292 photomultiplier tube in an evacuated holder. By special preparation of the CsI crystal and careful selection of a photomultiplier tube, an energy resolution of 1.3% for 124-MeV C^{12} ions was obtained.

The response of CsI for heavy ions as a function of energy has been given by Quinton *et al.*[17] It is quite nonlinear at low energies, but becomes linear above about 70 MeV, where these experiments were done. It has also been shown[8] that the pulse height is approximately the same for a C^{12} ion of 100 MeV and a C^{11} ion of 90 MeV. Thus, because of the large neutron binding energy in C^{12} (18.7 MeV), C^{11} ions produced in the (C^{12},C^{11}) single-neutron transfer reaction could have energies approximately 12 MeV lower than the elastically scattered C^{12} ions, and so produce pulses of nearly the same height. Therefore, in the later stages of the experiments, the CsI counter was replaced by a silicon-diffused junction detector. The response of the silicon detector is linear with energy, independent of the type of particle detected. The energy resolution was 1%. Some of the measurements taken with the CsI counter were repeated with the silicon detector, and the results agreed within the statistical errors. The detector pulses were amplified, then displayed on a PENCO 100-channel pulse-height analyzer. Since the linear accelerator is a pulsed machine with a macroscopic duty factor of 2–3%, the dead time of the analyzer had to be considered. During each 2-msec beam burst, the intensity had to be sufficiently low so that the dead time should not cause any large losses in counts. A maximum average counting rate of 600 per sec was therefore adopted. A correction was made in order to account for the nonuniform distribution of the incoming pulses. Figure 2 shows some typical energy spectra.

Target thicknesses near 1 mg/cm^2 were used so that the details in the structure of the angular distributions were not washed out, as might have been the case had an appreciable energy spread been introduced by thicker targets. Self-supporting Ta and Fe targets were made by rolling films down to the desired thickness with steel rolls. Ag^{107} and In films were made by vacuum deposition out of a tungsten crucible onto a glass plate. The films were stripped off the glass and mounted on brass rings. Ni films of 1.2 μ thickness were commercially available.[18]

[17] A. R. Quinton, C. E. Anderson, and W. J. Knox, Phys. Rev. **115**, 886 (1957).
[18] From McKay Company, New York.

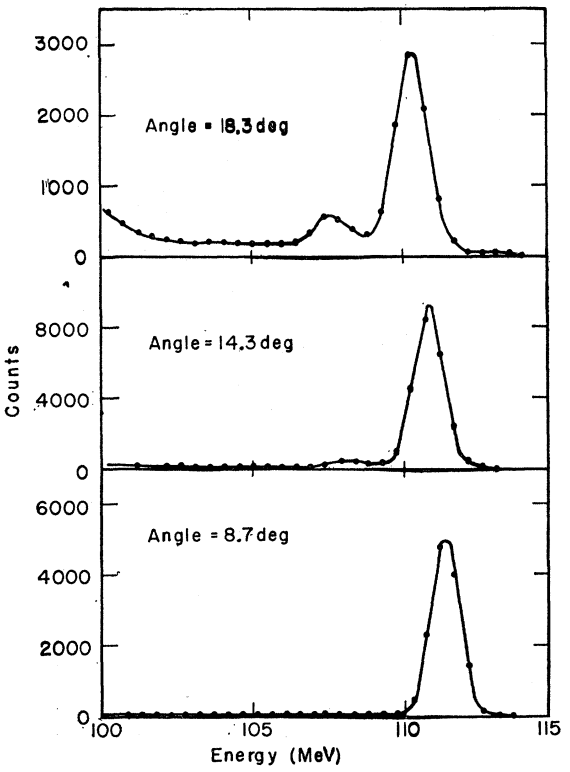

FIG. 2. Typical energy spectra taken with the CsI scintillation counter for C^{12} ions of 124.5 MeV scattered from Fe. The bump at larger angles is due to inelastic events.

The counters were moved manually, and the angular settings could be reproduced to within 0.1 deg. If the beam axis does not coincide with the chamber axis, a large error is introduced in the scattering angle, especially since measurements were taken at both sides of the chamber. An optical alignment system was therefore used every time both collimator sets (see Fig. 1) were changed. During each run, the alignment was further checked by measuring the cross section at 6, 7, and 8 deg on both sides of the chamber. The checks proved that the deviations were never larger than 0.1 deg. An angular spread is caused by the finite circular aperture of the counter collimator and the size of the circular beam spot on the target. Assuming that the beam density was constant over the beam area (which probably is very nearly correct, since the collimator selected only a small part of the center of the beam), the intensity distribution for the beam-spot–counter system was calculated by folding together the two separate distributions. The resulting distribution was nearly identical with a Gaussian distribution, with a standard deviation of 0.2 deg.

Multiple scattering at the chamber window adds to the spread calculated above. The root-mean-square angle for this multiple scattering was 0.5 deg for a typical case in our experiments. However, no correction was necessary because the number of particles that were

TABLE I. Experimental results: Fe+C^{12}. Target thickness $=2.4\pm0.04$ MeV; $\lambda=0.145$ F; $E_{c.m.}=102.5$ MeV; $n=7.69$.

$\theta_{c.m.}$ (deg)	$\left(\frac{d\sigma}{d\Omega}\right)/\left(\frac{d\sigma}{d\Omega}\right)_R$	Error (%)	$\theta_{c.m.}$ (deg)	$\left(\frac{d\sigma}{d\Omega}\right)/\left(\frac{d\sigma}{d\Omega}\right)_R$	Error (%)
6.4	0.982	3.5	18.5	0.139	1
7.6	0.933	1	19.7	0.101	1
8.9	1.140	1	20.9	0.0734	1
10.1	1.104	1	22.1	0.0507	1
11.3	0.961	1	23.7	0.0238	1.5
12.5	0.723	1	25.0	0.0183	1.5
13.7	0.561	1	26.2	0.0131	2.5
14.9	0.373	1	27.4	0.00885	3
16.1	0.302	1	28.6	0.00575	3.5
17.3	0.200	1			

scattered out of the detector solid angle due to multiple scattering in the windows were, to a good approximation, equal to those multiply scattered in. The contribution to the angular spread due to multiple scattering in the target could be neglected, but it set a lower limit of approximately 5 deg for the angle where the elastic scattering could be measured. At very small angles, a second-order correction had to be made, allowing for the large change in cross section over the angular region of detection.

TABLE II. Experimental results: Ni+C^{12}. Target thickness $=1.40\pm0.07$ MeV; $\lambda=0.144$ F; $E_{c.m.}=103.4$ MeV; $n=8.28$.

$\theta_{c.m.}$ (deg)	$\left(\frac{d\sigma}{d\Omega}\right)/\left(\frac{d\sigma}{d\Omega}\right)_R$	Error (%)	$\theta_{c.m.}$ (deg)	$\left(\frac{d\sigma}{d\Omega}\right)/\left(\frac{d\sigma}{d\Omega}\right)_R$	Error (%)
5.3	1.049	1	14.8	0.447	1
6.5	0.979	1	17.2	0.233	1
7.7	0.970	1	19.6	0.112	1.5
8.9	1.123	1	22.0	0.0533	1.5
9.1	1.133	1	23.4	0.0356	1.5
10.1	1.136	1	24.6	0.0253	1.5
10.3	1.190	1	25.8	0.0179	1.5
12.2	1.027	1	27.0	0.0137	2
12.4	0.810	1	28.2	0.0084	2
13.4	0.608				

TABLE III. Experimental results: Ag^{107}+C^{12}. Target thickness $=2.30\pm0.13$ MeV; $\lambda=0.133$ F; $E_{c.m.}=111.9$ MeV; $n=13.90$.

$\theta_{c.m.}$ (deg)	$\left(\frac{d\sigma}{d\Omega}\right)/\left(\frac{d\sigma}{d\Omega}\right)_R$	Error (%)	$\theta_{c.m.}$ (deg)	$\left(\frac{d\sigma}{d\Omega}\right)/\left(\frac{d\sigma}{d\Omega}\right)_R$	Error (%)
6.9	1.050	1	19.2	0.948	1
8.0	1.054	1	20.3	0.806	1
8.6	0.969	1	20.7	0.738	1
9.1	1.033	1	21.6	0.580	1
9.7	0.996	1	21.9	0.530	1
10.4	1.056	1	23.0	0.409	1
11.5	1.031	1	25.0	0.234	2
12.6	0.931	1	26.3	0.167	1
13.7	1.027	1	27.4	0.118	1.5
14.8	1.151	1	28.5	0.0842	1.5
16.0	1.279	1	29.6	0.0584	1.5
17.0	1.248	1	32.9	0.0331	2
18.2	1.177	1	34.0	0.0142	3
19.0	1.014	1	34.4	0.0133	1.5

In most cases, the differential cross sections have been divided by the Coulomb cross section and then normalized to unity by drawing a straight line through the average of the points close to zero degrees. This is justified by the fact that the cross sections oscillate slightly around the pure Coulomb scattering cross section for small angle scattering. The error introduced this way is at the most 2% and even less for heavy targets. In principle, the cross sections could be measured absolutely, but uncertainties in beam integration and target thicknesses precluded absolute determinations with probable errors of less than 5%. The above method of normalization was, therefore, chosen to represent the data, although, in some cases, both methods were used and found to agree within the experimental errors. For Fe, the above normalization could not be applied since the region of oscillations around Rutherford scattering could not be reached. Consequently, larger errors had to be assigned to the absolute cross sections in this case. The errors of points in the angular distribution relative to each other are, however, the same as in the other cases; i.e., the angular distribution curve as a whole can be moved up or down by several percent, but not the points separately.

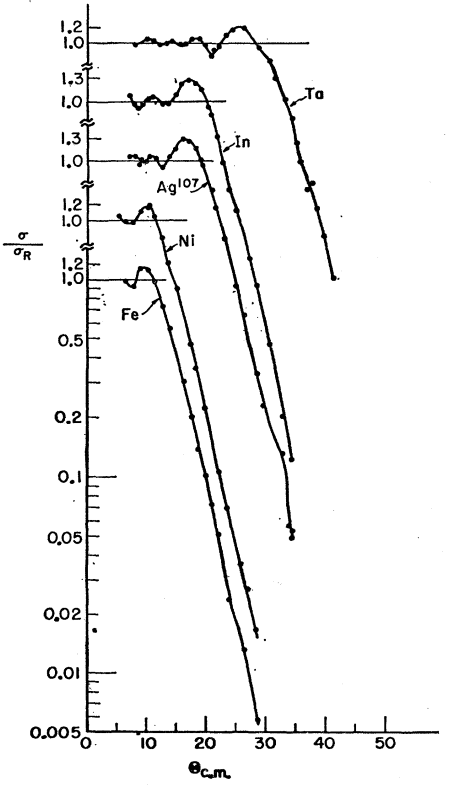

FIG. 3. Experimental angular distributions of C^{12} ions elastically scattered from Fe, Ni, Ag^{107}, In, and Ta.

TABLE IV. Experimental results: In+C^{12}. Target thickness $=1.9\pm0.2$ MeV; $\lambda\!\!\!^{-}=0.132$ F; $E_{c.m.}=112.7$ MeV; $n=14.49$.

$\theta_{c.m.}$ (deg)	$\left(\frac{d\sigma}{d\Omega}\right)/\left(\frac{d\sigma}{d\Omega}\right)_R$	Error (%)	$\theta_{c.m.}$ (deg)	$\left(\frac{d\sigma}{d\Omega}\right)/\left(\frac{d\sigma}{d\Omega}\right)_R$	Error (%)
7.1	1.069	1	19.2	1.113	1
8.2	0.960	1	20.3	0.937	1
8.4	0.933	1	20.8	0.855	1
9.3	0.964	1	21.7	0.663	1
9.5	0.981	1	22.8	0.469	1
10.4	1.023	1	23.9	0.359	1
11.6	1.030	1	25.0	0.282	1
12.7	0.989	1	27.2	0.155	1.5
13.8	0.983	1	28.3	0.117	3
14.8	1.085	1	30.5	0.589	3
15.9	1.245	1	32.7	0.0258	1.5
17.0	1.290	1	34.4	0.0152	4
18.1	1.231	1			

TABLE V. Experimental results: Ta+C^{12}. Target thickness $=2.6\pm0.3$ MeV; $\lambda\!\!\!^{-}=0.127$ F; $E_{c.m.}=116.9$ MeV; $n=21.59$.

$\theta_{c.m.}$ (deg)	$\left(\frac{d\sigma}{d\Omega}\right)/\left(\frac{d\sigma}{d\Omega}\right)_R$	Error (%)	$\theta_{c.m.}$ (deg)	$\left(\frac{d\sigma}{d\Omega}\right)/\left(\frac{d\sigma}{d\Omega}\right)_R$	Error (%)
7.9	0.99	1	25.3	1.29	1
9.0	1.01	1	26.3	1.25	1
10.2	1.01	1	27.4	1.22	1
11.2	0.98	1	28.5	1.09	1
12.2	0.96	1	29.5	0.94	1
13.3	0.97	1	30.6	0.81	1
14.4	1.01	1	31.6	0.67	1
15.5	0.98	1	33.3	0.46	3
16.5	0.99	1	34.3	0.38	1
17.6	1.04	1	34.9	0.312	1
18.7	1.05	1	35.8	0.250	1
19.7	0.98	1	37.6	0.166	1
20.9	0.91	1	38.7	0.122	2
22.1	0.96	1	39.6	0.103	3
23.2	1.09	1	41.2	0.063	3
24.2	1.19	1			

III. EXPERIMENTAL RESULTS AND ANALYSIS

The experimentally measured angular distributions are tabulated in Tables I to V and are also plotted in Fig. 3.

Column 1 gives the center-of-mass angle. The spread is ±0.7 deg.

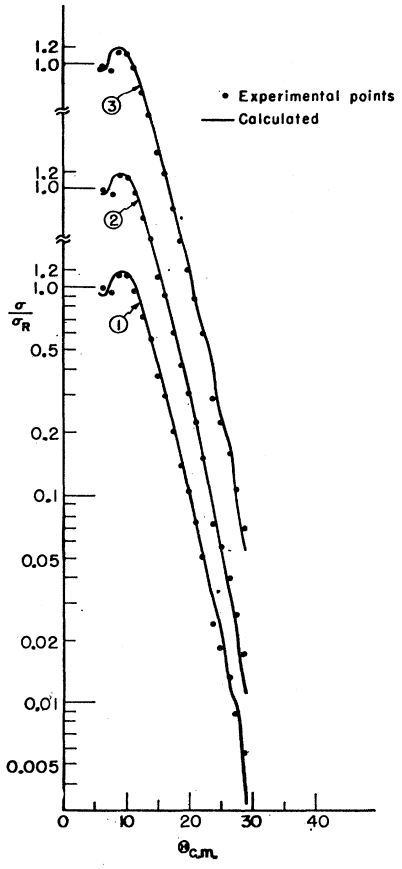

FIG. 4. Angular distributions of C^{12} ions elastically scattered from Fe at $E_{Lab}=124.5$ MeV. The data are the measured cross sections, and the solid line is the calculated cross section with the following parameter values:

	l_A	Δl_A	δ	l_δ	Δl_δ	Δ	$\sigma_{Reaction}(b)$
(1)	50	2.8	0.75	50	2.8	247	1.89
(2)	51	3.0	0.6	51	3.0	195	1.97
(3)	52	2.8	0.6	52	2.8	151	2.03.

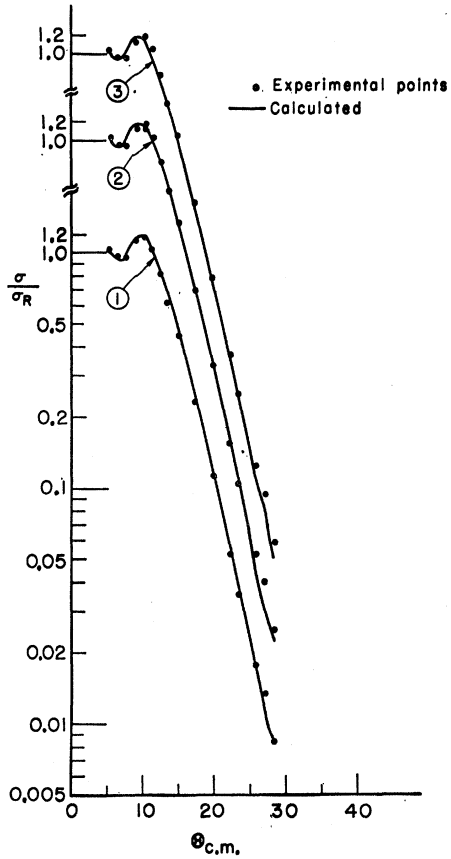

FIG. 5. Angular distributions of C^{12} ions elastically scattered from Ni at $E_{Lab}=124.5$ MeV. The data are the measured cross sections, and the solid line is the calculated cross section with the following parameter values:

	l_A	Δl_A	δ	l_δ	Δl_δ	Δ	$\sigma_{Reaction}(b)$
(1)	55	3.0	0.5	55	3.0	147	2.23
(2)	56	3.0	0.5	56	3.0	115	2.31
(3)	57	3.2	0.4	57	3.2	137	2.40.

Column 2 gives the measured cross section, normalized as discussed before. The cross sections are corrected for all the effects listed in the preceding section.

Column 3: The error includes the statistical error in the number of counts and the uncertainty in separating the elastic peak in the energy spectrum from the inelastic events (important only for large angles).

λ is the deBroglie wave length.

$n=Z_1Z_2e^2/\hbar v$ is the parameter characterizing Coulomb scattering.

Angular distributions calculated with Eq. (5) are shown in Figs. 4, 5, 6, 7, and 8, together with the experimental points. A value of Δ near the sum of statistical errors indicates a good fit between experiment and theory. All important features of the experimental angular distributions can be reproduced by using only three of the five available parameters, making $l_A=l_\delta$ and $\Delta l_A=\Delta l_\delta$. The large experimental initial rise for Ag^{107} and In was duplicated by making δ_l large. In most cases, $\Delta l_A\geq 2$; for $\Delta l_A<2$, strong oscillations appear again, although at larger angles than is the case in the sharp-cutoff model analyses. By varying all five parameters independently, refinements in the fits were made. The results derived from the analysis are tabulated in Table VI. Column 1 gives the absorption radius that is obtained by averaging the radii derived from all the possible l_A values. The error indicated is the maximum error corresponding to extreme values of l_A.

The r_a values listed in column 2 agree very well with those determined by Reynolds *et al.*,[5] in their "sharp cutoff" model analysis of the scattering of C^{12}, N^{14}, O^{16}, and Ne^{20} from Au^{197}, Bi^{209}, Pb^{206}, Pb^{207}, and Pb^{208}. The somewhat larger value for Ni in column 2 may be explained by the fact that no distinction in goodness of fit among four l_A values could be made in this case, thereby resulting in a rather large error.

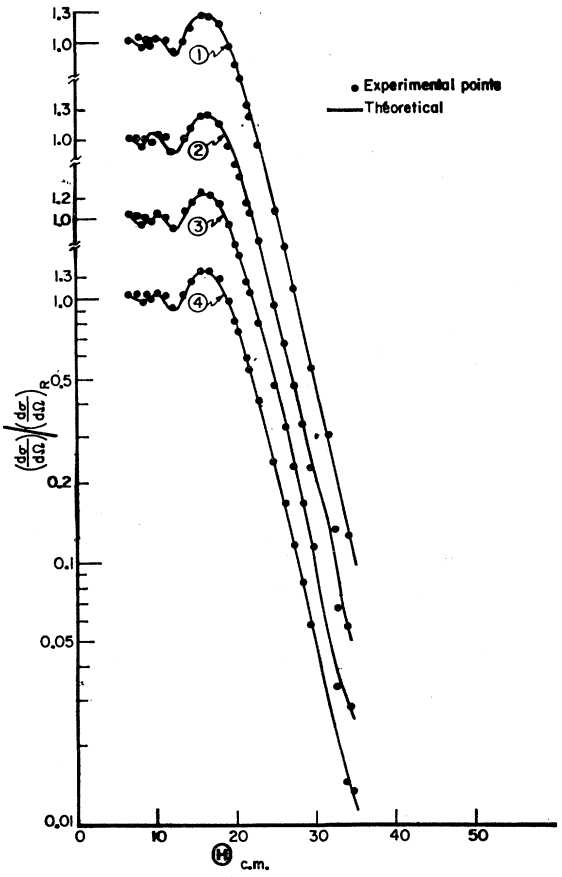

FIG. 6. Angular distributions of C^{12} ions elastically scattered from Ag^{107} at $E_{Lab}=124.5$ MeV. The data are the measured cross sections, and the solid line is the calculated cross section with the following parameter values:

	l_A	Δl_A	δ	l_δ	Δl_δ	Δ	$\sigma_{reaction}(b)$
(1)	60	2.2	0.7	61	3.0	162	2.18
(2)	60	2.4	0.9	60	2.5	151	2.19
(3)	61	2.6	0.8	61	2.0	153	2.28
(4)	61	2.8	0.9	60	2.5	146	2.29.

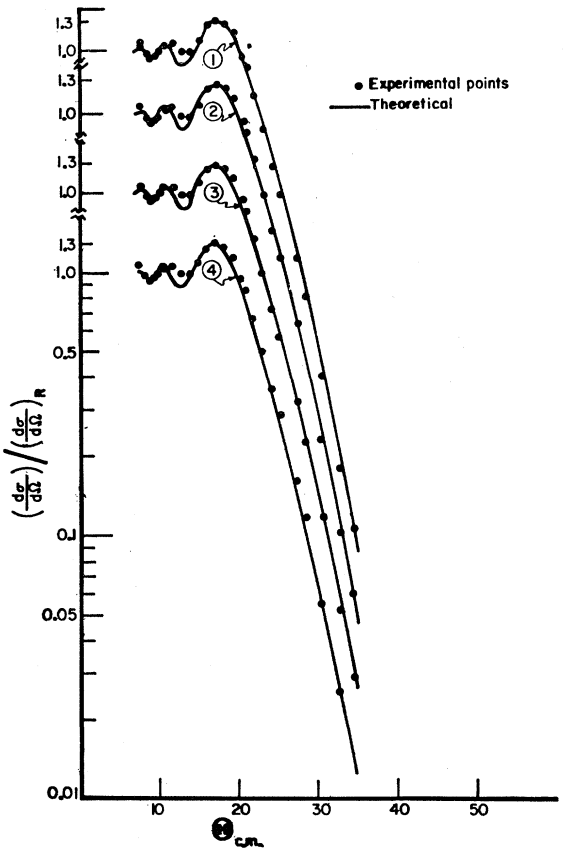

FIG. 7. Angular distributions of C^{12} ions elastically scattered from In at $E_{Lab}=124.5$ MeV. The data are the measured cross sections, and the solid line is the calculated cross section with the following parameter values:

	l_A	Δl_A	δ	l_δ	Δl_δ	Δ	$\sigma_{reaction}(b)$
(1)	61	2.4	0.8	61	3.2	153	2.23
(2)	61	2.0	0.8	62	2.5	155	2.20
(3)	62	2.3	0.6	63	2.5	200	2.29
(4)	62	2.2	1.0	61	3.0	208	2.29.

Column 3 gives the absorption surface parameter t, obtained from the average values of Δl_A.

The reaction cross sections, given by

$$\sigma_R=\frac{\pi}{k^2}\sum_{l=0}^{\infty}(2l+1)(1-A_l^2) \tag{6}$$

and listed in column 4, were obtained by averaging the values given by all the possible l_A and Δl_A values. These cross sections agree very well with those calculated from the expression[19]

$$\sigma_R\simeq\pi(R+\lambda)^2\left[1-\frac{Z_1Z_2e^2}{(R+\lambda)E}\right],$$

with the value of R taken to be the absorption radius R_a.

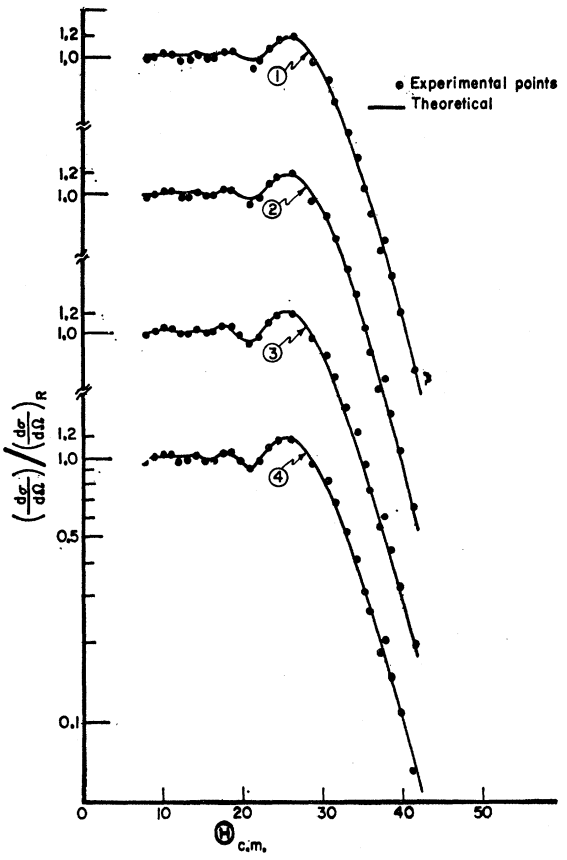

FIG. 8. Angular distributions of C^{12} ions elastically scattered from Ta at $E_{Lab}=124.5$ MeV. The data are the measured cross sections, and the solid line is the calculated cross section with the following parameter values:

	l_A	Δl_A	δ	l_δ	Δl_δ	Δ	$\sigma_{Reaction}(b)$
(1)	65	3.6	0.3	65	3.0	92	2.44
(2)	65	3.3	0.3	66	2.6	82	2.42
(3)	66	2.7	0.3	66	2.7	109	2.44
(4)	66	3.0	0.3	66	2.0	90	2.46.

[19] J. M. Blatt and V. F. Weisskopf, *Theoretical Nuclear Physics* (John Wiley & Sons, Inc., New York, 1952).

TABLE VI. Results derived from phase-shift analysis.

	R_a (F)	$r_a=\frac{R_a}{A_1^{1/3}+A_2^{1/3}}$ (F)	t (F)	$\sigma_{reaction}$ (b)
Fe	8.65±0.20	1.42±0.02	0.43±0.06	2.14±0.10
Ni	9.32±0.30	1.51±0.05	0.44±0.05	2.29±0.15
Ag^{107}	10.15±0.12	1.44±0.02	0.31±0.05	2.23±0.07
In	10.30±0.12	1.44±0.02	0.27±0.04	2.20±0.05
Ta	11.57±0.14	1.45±0.02	0.37±0.09	2.43±0.03

IV. DISCUSSION

One should note that strong absorption can result in an absorption radius R_a substantially larger than the complex potential well radius, usually taken to be slightly larger than that of the nuclear density. This follows from the fact that complex particles can be absorbed (i.e., removed from the entrance channel) when they interact with the outermost low-density nuclear region. A correspondingly smaller absorption surface thickness parameter t will result. This is illustrated in Fig. 9, where a typical complex potential radial form $f(r)$ characterized by a radius parameter r_0 and a surface thickness parameter a is compared with an $A_l(r)$ determined from our C^{12}+Ta scattering data. Since $R=r_0(A_1^{1/3}+A_2^{1/3})$ is the value of r at which $f(r)=\frac{1}{2}$, whereas $R_a=r_a(A_1^{1/3}+A_2^{1/3})$ is the distance of closest approach for which absorption is 75% (fractional absorption$=1-A_l^2=\frac{3}{4}$), an $r_0=r_a$ would be purely fortuitous. Thus, the substantial differences between $r_a=1.45$ F and $r_0=1.30$ F and between $t=0.37$ F and $a=0.55$ F are explained.

Recently, the parameterization of A_l given by (2) has been qualitatively justified, and that of δ_l examined.[8,10] It was concluded that the form (2) of δ_l was incorrect, but that a parameterization having at least qualitative theoretical justification gave approximately the same results in the analysis of our C^{12}+Ta data. This was seen to be due to the fact that in the region of smaller l values, where the two δ_l forms differ appreciably, $A_l\to 0$ so that little change was made in the scattering amplitude. For analysis of the scattering of less strongly absorbed particles, however, a theoretically proper form of δ_l should be necessary.

Even though parameterized phase-shift analyses can provide precise values of absorption radii and surface

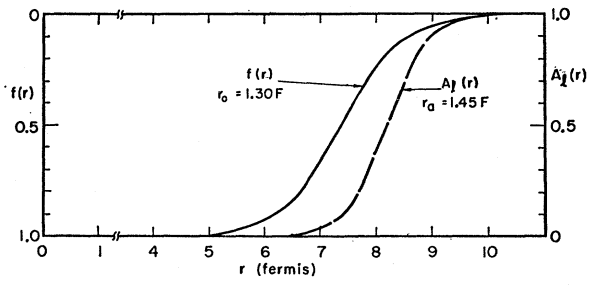

FIG. 9. An optical-model potential $f(r)$ compared with $A_l(r)$.

thicknesses, it has been pointed out that precise analyses are meaningful only when the elastic scattering can be cleanly separated from inelastic events,[7] or when correction for the inelastic contribution can be made.[20]

[20] A. Isoya, H. E. Conzett, E. Hadjimichael, and E. Shield, in *Proceedings of the Third Conference on Reactions between Complex Nuclei*, edited by A. Ghiorso, R. M. Diamond, and H. E. Conzett (University of California Press, Berkeley, 1963), paper A9.

ACKNOWLEDGMENTS

We would like to thank Dr. B. G. Harvey, Dr. I. Perlman, and Dr. J. O. Rasmussen for their interest in this work. We are grateful to Jack H. Elliott for the manufacturing of the silicon diffused junction detectors and to David O'Connell for preparation of the Ag^{107} and In foils.

PHYSICAL REVIEW VOLUME 136, NUMBER 4B 23 NOVEMBER 1964

Quasifree Electron-Proton Scattering in H^3 and He^3†

ARNE JOHANSSON*
High Energy Physics Laboratory, Stanford University, Stanford, California
(Received 29 June 1964)

Measurements have been made of the cross sections of coincidences between scattered electrons and ejected protons, when targets of H^3 and He^3 are bombarded with 550-MeV electrons. The variation of the cross section with proton angle and proton energy has been studied for fixed electron angle and energy. The results are compared with theoretical calculations based on different three-body nuclear wave functions.

I. INTRODUCTION

RECENTLY there has been considerable interest, both theoretical and experimental, in the study of the three-body nuclei.[1] In the present paper, we would like to report results of a scattering experiment which, in principle at least, is quite sensitive to the wave function of a proton inside the nucleus. High-energy electrons are used as incident particles and the experiment consists of the detection in coincidence of a scattered electron and a knockout proton, which has been given a comparatively large momentum by the electron. The fact that only protons of large momentum are considered means that the process can be viewed as a free collision inside the nucleus between an electron and a proton. The principal effect of the nuclear wave function is felt through the momentum distribution of the proton before the collision. This momentum distribution will reveal itself in the angular correlation distribution between the scattered electron and the proton. The energy required to break up the initial nucleus depends on the state of the two spectator particles. Thus in order to study the momentum distribution, i.e., the wave function, of protons coupled to various states of the other two nucleons one has to perform the experiment with good angular resolution as well as good energy resolution.

This experiment is similar to the quasifree scattering of protons on protons in various nuclei, a process which has been studied at several laboratories during the last few years.[2] It has been suggested by Jacob and Maris[3] that the same kind of study might be done using electrons as the incident particles rather than protons. The advantages would be that the electrons are far less distorted by the nuclear field than are the strongly interacting protons. The main drawback is the very low cross section in the electron case and the poor duty-cycle of existing electron accelerators. The present experiment is the first attempt to use electrons for such studies[4] and, besides offering an interesting study, the nuclei H^3 and He^3 have comparatively high cross sections and low background due to uncorrelated events.

II. THEORY

A calculation of the coincidence cross section as a function of proton angle when the electron energy and angle are kept fixed has been done by Griffy and Oakes[5] using the impulse approximation. We will only make a few remarks about the kinematics of the reactions.

We assume that the electron interacts only with the

† This work was supported in part by the U. S. Office of Naval Research, the Air Force Office of Scientific Research, and the Atomic Energy Commission through Los Alamos Scientific Laboratory. Computations were supported by the National Science Foundation.

* Present address: Gustaf Werner Institute, Uppsala, Sweden.

[1] See, for instance, a. J. M. Blatt and L. M. Delves, Phys. Rev. Letters **12**, 544 (1964). b. L. I. Schiff, Phys. Rev. **133**, B802 (1964). c. J. S. Levinger and T. L. Chow, Bull. Am. Phys. Soc. **9**, 465 (1964). d. H. Collard, R. Hofstadter, A. Johansson, R. Parks *et al.*, Phys. Rev. Letters **11**, 132 (1963).

[2] See, for instance, G. Tibell, O. Sundberg, and P. U. Renberg, Arkiv Fysik **25**, 433 (1963), where further references are given.

[3] G. Jacob and Th. A. J. Maris, Nucl. Phys. **31**, 139 (1962); **31**, 152 (1962).

[4] M. Croissiaux [Phys. Rev. **127**, 613 (1962)] and D. Aitken [Ph.D. thesis, Stanford University, 1964 (unpublished)] have measured electron-proton coincidences from the reaction $e+d \rightarrow e'+p+n$ with the principal objective of determining the form factor of the bound proton.

[5] T. A. Griffy and R. J. Oakes, Phys. Rev. **135**, B1161 (1964).